Mechanism of the Photodegradation of A-D-A Acceptors for Organic Photovoltaics

Yuxuan Che,[a] Rizwan Niazi,[a] Ricardo Izquierdo,[b] and Dmitrii F. Perepichka*,[a]
a) Department of Chemistry, McGill University, Montreal, Quebec H3A 0B8, Canada
b) Department of Electrical Engineering, École de Technologie Supérieure, Université du Québec, Montréal, Québec H3C 1K3, Canada
*Dmitrii.perepichka@mcgill.ca

In this work, we elucidate the photodegradation pathway of IT-4F, a benchmark A-D-A type semiconductor for organic photovoltaics. The photoproducts were isolated and shown to be isomers of IT-4F formed via a 6-*e* electrocyclic reaction between the dicyanomethylene unit and the thiophene ring, followed by a 1,5-sigmatropic hydride shift. Importantly, this photoisomerization is accelerated under inert conditions which is explained by DFT calculations that predict the reaction to occur via the excited triplet state (quenchable by oxygen). Adding controlled amounts of the photocyclized product P1 to PM6:IT-4F bulk heterojunction cells shows a progressive decrease of photocurrent and fill factor attributed to its poorer absorption and charge transport properties. The power conversion efficiency drops from 12% for pure IT-4F to 3% for pure P1 acceptor. This cyclization is a general photodegradation pathway for a series of analogous A-D-A molecules with 1,1-dicyanomethylene-3-indanone termini. However, the rate of the reaction varies widely with the nature of the donor moiety.

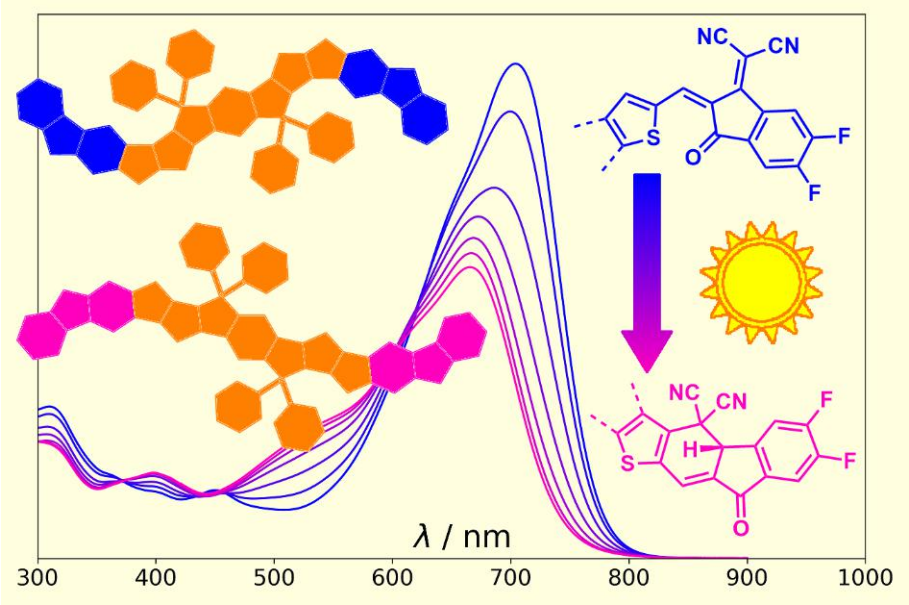

The past decade has seen a remarkable progress in the field of organic photovoltaics (OPVs) holding the promise of clean, low-cost and renewable energy sources.[1,2,3,4] The greatly improved device performance is mainly attributed to the design of new semiconducting materials. In particular, the use of nonfullerene acceptors (NFAs) enhances light absorption and expands spectral coverage, resulting in significantly higher photocurrent compared to conventional fullerene cells.[5,6] Furthermore, the structural diversity of NFAs offers excellent synthetic flexibility and tunability, realizing a wide range of structures with highly optimized electronic characteristics.[7,8,9,10] Among all NFAs, the acceptor-donor-acceptor (A-D-A) architecture has proven to be the most successful, owing to high absorptivity in the visible and near-infrared (NIR) region and a special solid state packing with 3D π-π interactions that lead to efficient charge transport.[11,12,13,14] The emergence of new A-D-A structures including IT-series[15,16,17] and Y-series[18,19,20] has pushed the power conversion efficiency (PCE) beyond 18% in single-junction organic solar cells, closing the gap with inorganic photovoltaic technologies.

Despite these breakthrough performance of NFA-based OPVs, their stability is typically lower than that of fullerene-based devices, and remains a major hurdle for commercialization.[21,22] Among many factors (such as morphological change), photodegradation of the active layer material plays a crucial role in the deterioration of device performance, yet relatively little effort was devoted to understanding its mechanism.[23,24] Several degradation pathways were proposed in the past. Most of these assume photooxidation as the key mechanism,[25,26] although photocatalytic degradations of the vinylene bridge at the interface (with ZnO electron extraction layer) have also been proposed.[27,28,29] However, no unambiguous identifications of degradation products have been reported, and this limited understanding of the molecular origin of degradation remains a key challenge for improving the stability of OPVs.[30,31] Here, we uncover a new mechanism of the photodegradation of A-D-A NFAs which is based on intramolecular cyclization involving the 1,1-dicyanomethylene-3-indanone (INCN) moiety. As an isomerization reaction, it cannot be suppressed by eliminating oxygen (with antioxidants or encapsulations) but can be effectively mitigated by the structural design of the A-D-A molecule.

We have chosen **IT-4F** as one of the current benchmarks in OPVs: it's (fluorinated) INCN termini have recently become the most popular acceptor group in the community (Fig. S1). The material was subjected to intense illumination in preparative scale to obtain sufficient amounts of

photoproducts for detailed structural analysis, optical characterizations and device studies. During this process, two major higher-polarity products were formed sequentially (Fig. 1a) and were isolated via column chromatography. MALDI-MS shows the molecular weight of both species identical to **IT-4F**, confirming their isomeric nature (Fig. 1b). Their molecular structures were determined with ^{1}H and ^{13}C NMR (including 2D correlation) spectroscopy (Fig. S9~S16), and the proposed mechanism of reaction involving *cis-trans* isomerization (**1**→**2**), electrocyclic reaction (**2**→**3**) and sigmatropic shift (**3**→**4**) is shown in Scheme 1.

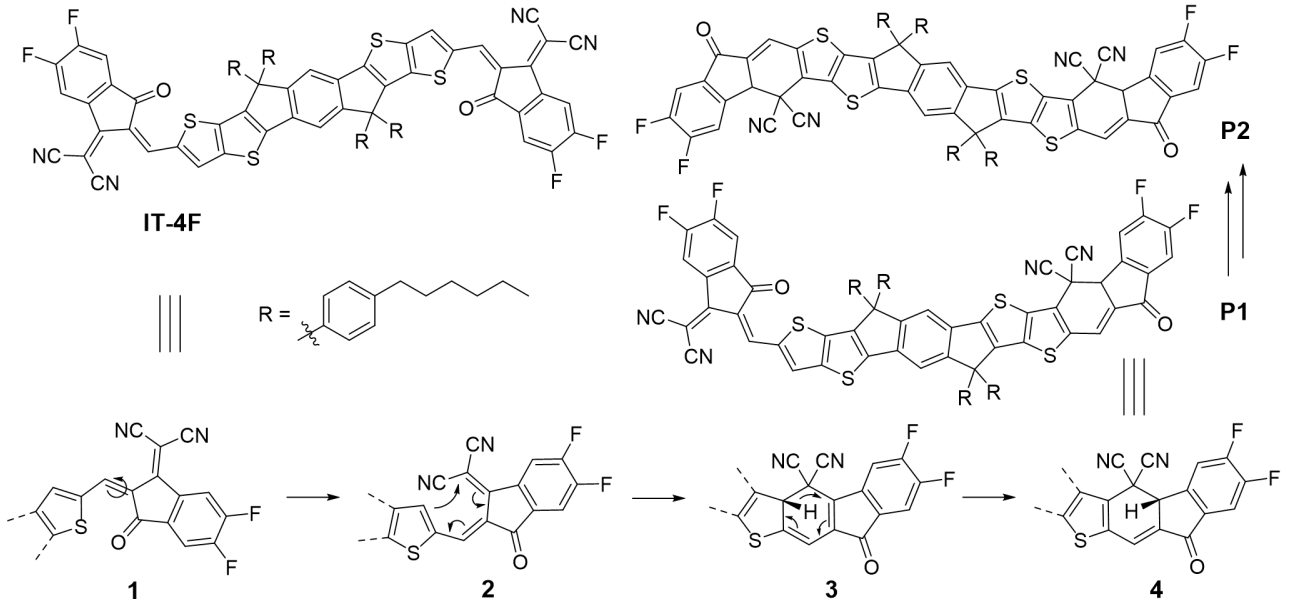

Scheme 1. Mechanism of the photodegradation of **IT-4F**.

The first degradation product (**P1**) is an asymmetric isomer of **IT-4F** resulting from an electrocyclic ring closure involving one terminal INCN moiety, and a subsequent 1,5-hydride shift which restores the conjugation across the backbone. A similar process on the second INCN moiety leads to the fully fused **P2**. Formed by reversible aldol condensation, the vinylene bond bridging the donor and acceptor moieties was often speculated to be the origin of the photoinduced decomposition of IT-series and many other A-D-A type NFAs.[26,27,29] However, our results unequivocally show that the photodegradation involves the dicyanomethylene moiety, while the vinylene bridge is not the immediate reaction center. The ^{1}H NMR spectrum of both degradation products features an sp^3 singlet at ~4.7 ppm (Fig. S2), which was also observed in a recent photostability study and attributed to the formation of epoxides upon photooxidation of the vinylene bridge.[26] However, the corresponding ^{13}C chemical shift of the degradation product we obtained (~45 ppm, Fig. S14) is not consistent with that for epoxides, which is expected to be >55

ppm. Being isomers of **IT-4F**, **P1** and **P2** are undetectable via MS which is commonly applied in mechanistic studies of OPV photodegradation. Importantly, this process does not involve oxygen or water and even proceeds at a slightly faster rate under an inert atmosphere (Fig. 3).

Compared to **IT-4F**, the absorption maxima of **P1** and **P2** are blue-shifted by 45 nm (0.13 eV) and 164 nm (0.57 eV), respectively (Fig. 1c and Table S1). This shift of the intramolecular charge transfer band is explained by the decoupling of the strongest acceptor moiety (dicyanomethylene) from the donor core. A similar trend is also found in the emission spectra. However, while **IT-4F** and the intermediate **P1** are only weakly emissive, **P2** gives a very high photoluminescence quantum yield (PLQY) of 73%. The dramatically enhanced fluorescence of **P2** may be attributed to more rigid backbone and reduced rotational relaxation.

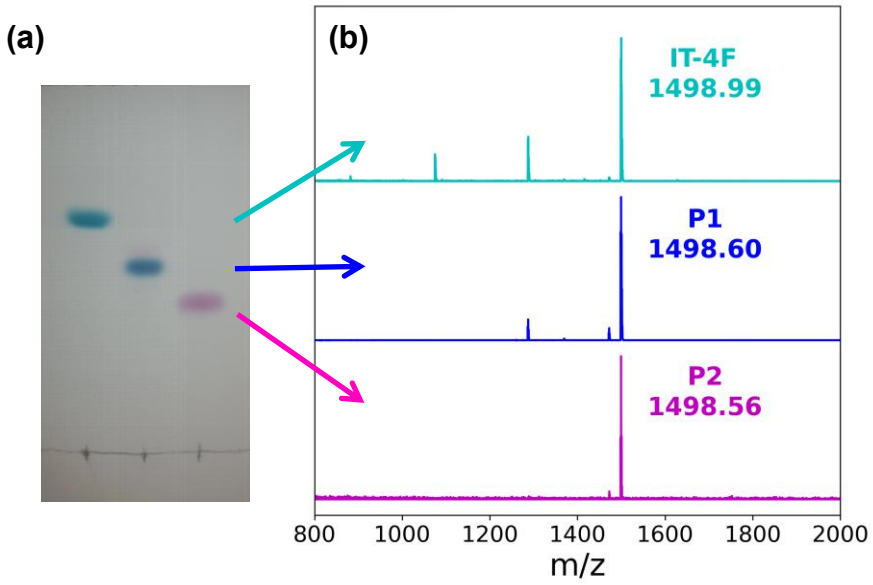

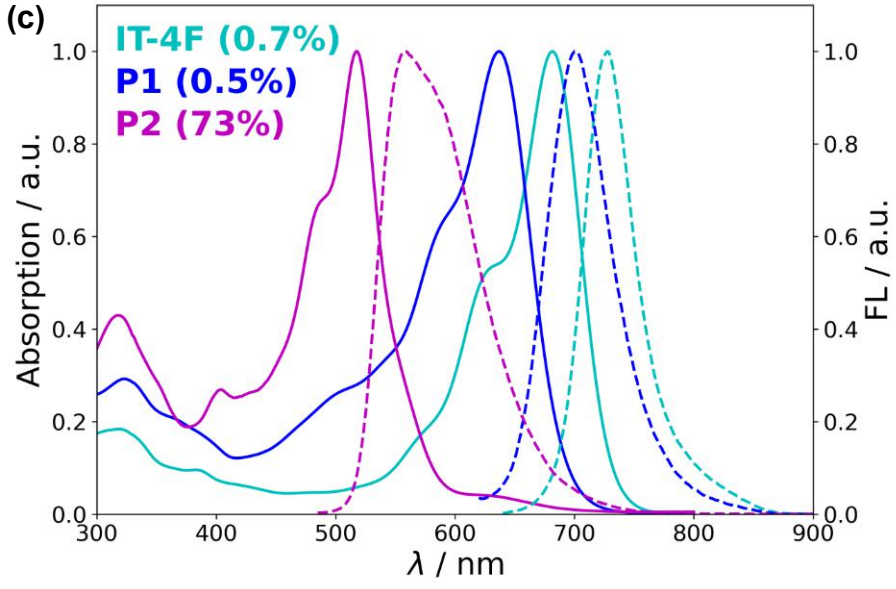

Figure 1. (a) Thin-layer chromatography, (b) MALDI-MS and (c) UV-Vis absorption (solid) and fluorescence (dashed) spectra and PLQY (in brackets) in chlorobenzene solutions for **IT-4F**, **P1** and **P2**. The absorption shoulder of **P2** >600 nm is due to residual amount of **P1**.

To support the proposed mechanistic hypothesis, we performed DFT calculations to find the transition states along the proposed reaction path (Fig. 2). First, the initial structure (**1**) must undergo a *cis-trans* isomerization of the vinylene bridge to adopt proper orientation of the terminal group (**2**). This isomerization was already suggested to be the initial step of the photodegradation in related INCN derivatives although its exact role was not fully understood.[26] The activation energy for the electrocyclic ring closure (**2-3**) in the singlet state (S_0, 35 kcal mol^{-1}) is too high for a thermally driven reaction at this temperature. However, a much lower barrier of 19 kcal mol^{-1} was calculated in the triplet state (T_1), as expected for a photo-driven transition. Although a large activation barrier (41 kcal mol^{-1}) is predicted for the subsequent 1,5-hydride shift (**3-4**) along the adiabatic ($T_1 \rightarrow T_1$) path, an intersystem crossing from intermediate **3** may achieve the transition to the ground state product at a cost of <10 kcal mol^{-1} (dashed curve). The electrocyclic reaction being the rate-limiting step is in line with the fact that intermediate **3** was not experimentally observed.

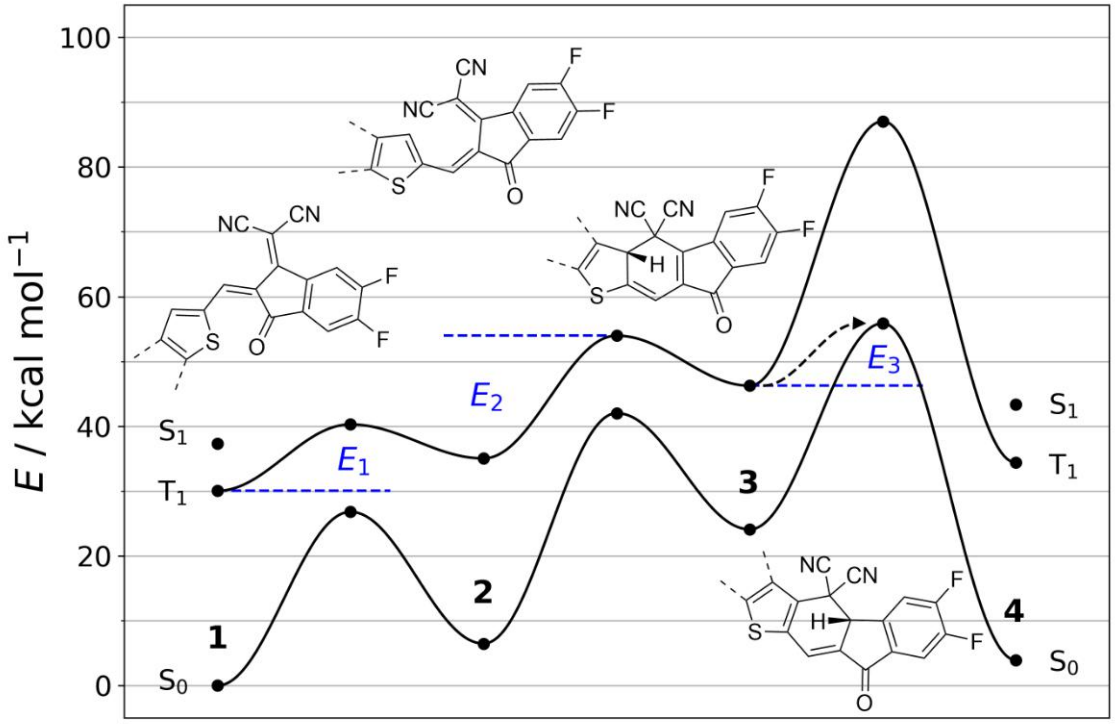

Figure 2. DFT [B3LYP/6-31G(d), IEFPCM, chlorobenzene] predicted energy surface along the proposed reaction path.

Predictably, restricted molecular motions in the solid state suppress the photocyclization of **IT-4F** under similar illumination conditions: >50% degradation was observed only after ~5 days (as compared to <1 h in solution). Further deceleration of the reaction in PM6:**IT-4F** blends (35% conversion after 8 days, Fig. S3) could be explained by the photoinduced electron transfer depopulating the reactive excited state. In both cases the formation of **P1** in thin films was confirmed spectroscopically (characteristic absorption at ~650 nm) and chromatographically (Fig. S4). This indicates that the photocyclization reaction is of prime importance to OPV devices, where oxygen concentration is typically low.

Bulk heterojunction OPV cells with PM6 (Scheme S1) as the donor polymer were fabricated to examine the implication of the formation of **P1** on device performance (Table 1 and Fig. S5). Already at 1:1 **IT-4F**:**P1** ratio, the PCE drops from 12% to ~9%, and it further deteriorates to ~3% for pure PM6:**P1** blends. This drop of performance largely originates from the drop of short-circuit current density (J_{SC}) and fill factor (FF). The lower NIR absorption of **P1**, as well as the steric hindrance from the protruding cyano groups leading to weaker intermolecular π-π interactions and lower electron mobility, are the two possible reasons for the observed changes.

Table 1. Effect of **P1** on the performance of Glass/ITO/PEDOT:PSS/Blend/PDINN/Ag cells.

PM6 : **IT-4F** : **P1**	V_{OC} / V	J_{SC} / mA cm^{-2}	FF / %	PCE / %
0.5 : 0.5 : 0	0.91 ± 0.01	19.3 ± 0.3	69 ± 1	12.0 ± 0.3
0.5 : 0.25 : 0.25	0.92 ± 0.01	16.3 ± 0.4	59 ± 1	8.9 ± 0.3
0.5 : 0 : 0.5	0.89 ± 0.02	9.4 ± 0.6	36 ± 2	3.1 ± 0.2

We tested the photostability of a similar NFA, previously reported **IDTT-4F** with non-fused backbone,[32] as shown in Scheme 2. **IDTT-4F** showed similar degradation pathway (Fig. S6) but much higher photostability (Fig. 3 and Fig. S7). The predicted activation energy for its electrocyclic reaction (~21 kcal mol^{-1}) is 2 kcal mol^{-1} higher than that of **IT-4F**, as shown in Table 2. The difference could be explained by the fact that the formation of intermediate **3** for **IDTT-4F** results in a full loss of aromaticity of the thiophene ring, while for **IT-4F** it transforms the 10-*e* thienothiophene into 6-*e* aromatic thiophene. The observed accelerated photodegradation of **IDTT-4F** in nitrogen-purged solutions, attributed to reduced triplet annihilation in the absence of oxygen, further supports the triplet-mediated reaction path. Originally introduced to increase the conformational specificity of the terminal group as well as the solubility,[33,34] alkyl side chains on

the outer positions of the electron-donating core are also important for the photostability of A-D-A NFAs. The steric hindrance of the alkyl group leads to a higher transition barrier for the electrocyclic ring closure. More importantly, much higher activation energy is required for the subsequent sigmatropic shift of the alkyl group, effectively blocking the reaction path. Overall, the predicted transition state energies along the reaction path are in full agreement with the observed rates of photodegradation.

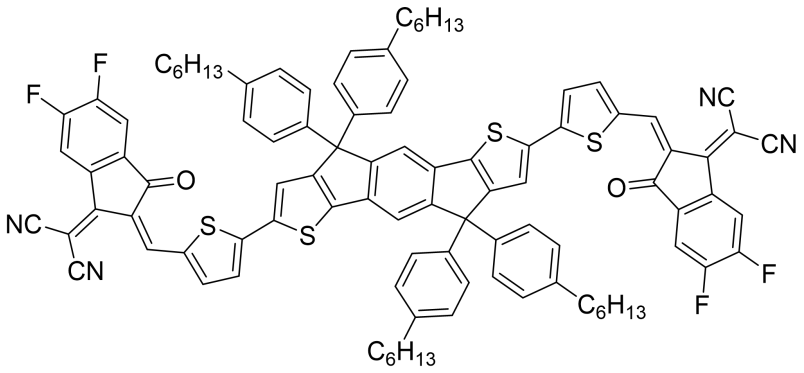

Scheme 2. Structure of **IDTT-4F**.

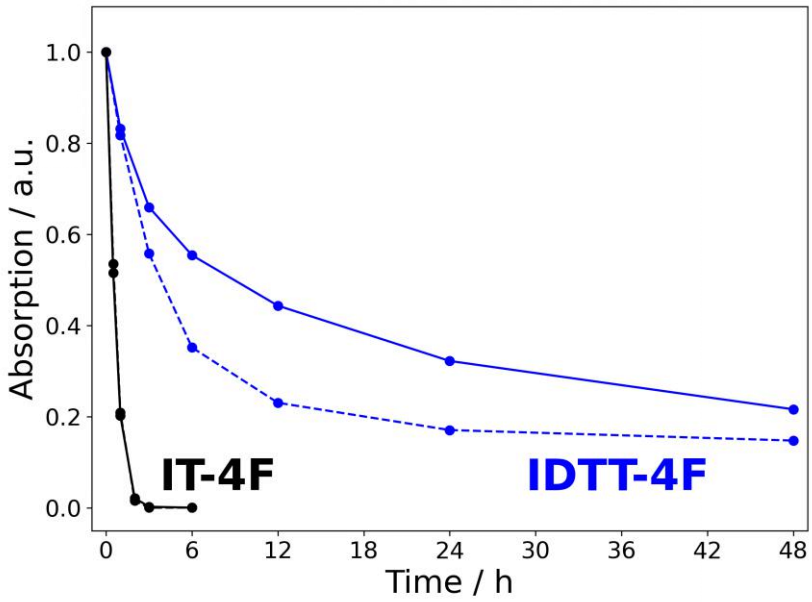

Figure 3. Photodegradation of **IT-4F** and **IDTT-4F** in chlorobenzene (initial optical density ~2.5) purged with air (solid) or nitrogen (dashed), as shown with the decay of normalized optical density at their wavelengths of half-maximum absorbance under the illumination of a 250 W tungsten halogen lamp (~10 lm cm^{-2}).

Table 2. DFT calculated activation energies along the reaction path for **IT-4F and IDTT-4F**.

E_a / kcal mol^{-1}	**1-2**	**2-3**	**3-4**
IT-4F	10.2	18.9	9.6
IDTT-4F	12.8	21.1	7.9

In conclusion, we have shown that the photodegradation of **IT-4F** and **IDTT-4F** involves intramolecular 6-*e* electrocyclic reactions producing fused-ring isomers which are not detectable by MS analysis. The reaction occurs via a triplet state and is slowed down in the presence of oxygen and electron donors due to the depopulation of the triplet state via energy and electron transfer. The rate of degradation depends on the structure of the outer ring of the donor moiety where thienothiophene > thiophene. This trend is in agreement with DFT calculated activation energies along the reaction path. While other degradation pathways in A-D-A containing OPVs are certainly possible and might even be dominant in some systems, we expect our work to inform the future molecular design of organic semiconductors with greatly improved photostability.

Acknowledgment
This work was supported by grants from NSERC, FRQNT and Quebec Center for Advanced Materials (QCAM). YC acknowledges a doctoral scholarship from FRQNT. The authors thank Cory Ruchlin for the help with PLQY measurements.

Reference

[1] Mishra, A.; Bäuerle, P. Small Molecule Organic Semiconductors on the Move: Promises for Future Solar Energy Technology. *Angew. Chem. Int. Ed.* **2012,** *51,* 2020–2067.
[2] Heeger, A. J. 25th Anniversary Article: Bulk Heterojunction Solar Cells: Understanding the Mechanism of Operation. *Adv. Mater.* **2014,** *26,* 10–28.
[3] Mazzio, K. A.; Luscombe, C. K. The future of organic photovoltaics. *Chem. Soc. Rev.* **2015,** *44,* 78–90.
[4] Inganäs, O. Organic Photovoltaics over Three Decades. *Adv. Mater.* **2018,** *30,* 1800388.
[5] Hou, J.; Inganäs, O.; Friend, R. H.; Gao, F. Organic solar cells based on non-fullerene acceptors. *Nat. Mater.* **2018,** *17,* 119–128.
[6] Zhang, J.; Tan, H. S.; Guo, X.; Facchetti, A.; Yan, H. Material insights and challenges for non-fullerene organic solar cells based on small molecular acceptors. *Nat. Energy* **2018,** *3,* 720–731.
[7] Zhang, G.; Zhao, J.; Chow, P. C. Y.; Jiang, K.; Zhang, J.; Zhu, Z.; Zhang, J.; Huang, F.; Yan, H. Nonfullerene Acceptor Molecules for Bulk Heterojunction Organic Solar Cells. *Chem. Rev.* **2018,** *118,* 3447–3507.
[8] Wadsworth, A.; Moser, M.; Marks, A.; Little, M. S.; Gasparini, N.; Brabec, C. J.; Baran, D.; McCulloch, I. Critical review of the molecular design progress in non-fullerene electron acceptors towards commercially viable organic solar cells. *Chem. Soc. Rev.* **2019,** *48,* 1596–1625.
[9] Cheng, P.; Li, G.; Zhan, X.; Yang, Y. Next-generation organic photovoltaics based on non-fullerene acceptors. *Nat. Photon.* **2018,** *12,* 131–142.
[10] Yan, C.; Barlow, S.; Wang, Z.; Yan, H.; Jen, A. K.-Y.; Marder, S. R.; Zhan, X. Non-fullerene acceptors for organic solar cells. *Nat. Rev. Mater.* **2018,** *3,* 18003.
[11] Wan, X.; Li, C.; Zhang, M.; Chen, Y. Acceptor–donor–acceptor type molecules for high performance organic photovoltaics – chemistry and mechanism. *Chem. Soc. Rev.* **2020,** *49,*

2828–2842.
[12] Yue, Q.; Liu, W.; Zhu, X. n-Type Molecular Photovoltaic Materials: Design Strategies and Device Applications. *J. Am. Chem. Soc.* **2020,** *142,* 11613–11628.
[13] Lai, H.; He, F. Crystal Engineering in Organic Photovoltaic Acceptors: A 3D Network Approach. *Adv. Energy Mater.* **2020,** *10,* 2002678.
[14] Liu, W.; Xu, X.; Yuan, J.; Leclerc, M.; Zou, Y.; Li, Y. Low-Bandgap Non-fullerene Acceptors Enabling High-Performance Organic Solar Cells. *ACS Energy Lett.* **2021,** *6,* 598–608.
[15] Lin, Y.; Wang, J.; Zhang, Z.-G.; Bai, H.; Li, Y.; Zhu, D.; Zhan, X. An Electron Acceptor Challenging Fullerenes for Efficient Polymer Solar Cells. *Adv. Mater.* **2015,** *27,* 1170–1174.
[16] Zhao, W.; Li, S.; Yao, H.; Zhang, S.; Zhang, Y.; Yang, B.; Hou, J. Molecular Optimization Enables over 13% Efficiency in Organic Solar Cells. *J. Am. Chem. Soc.* **2017,** *139,* 7148–7151.
[17] Zhang, H.; Yao, H.; Hou, J.; Zhu, J.; Zhang, J.; Li, W.; Yu, R.; Gao, B.; Zhang, S.; Hou, J. Over 14% Efficiency in Organic Solar Cells Enabled by Chlorinated Nonfullerene Small-Molecule Acceptors. *Adv. Mater.* **2018,** *30,* 1800613.
[18] Yuan, J.; Zhang, Y.; Zhou, L.; Zhang, G.; Yip, H.-L.; Lau, T.-K.; Lu, X.; Zhu, C.; Peng, H.; Johnson, P. A.; Leclerc, M.; Cao, Y.; Ulanski, J.; Li, Y.; Zou, Y. Single-Junction Organic Solar Cell with over 15% Efficiency Using Fused-Ring Acceptor with Electron-Deficient Core. *Joule* **2019,** *3,* 1140–1151.
[19] Cui, Y.; Yao, H.; Zhang, J.; Zhang, T.; Wang, Y.; Hong, L.; Xian, K.; Xu, B.; Zhang, S.; Peng, J.; Wei, Z.; Gao, F.; Hou, J. Over 16% efficiency organic photovoltaic cells enabled by a chlorinated acceptor with increased open-circuit voltages. *Nat. Commun.* **2019,** *10,* 2515.
[20] Liu, Q.; Jiang, Y.; Jin, K.; Qin, J.; Xu, J.; Li, W.; Xiong, J.; Liu, J.; Xiao, Z.; Sun, K.; Yang, S.; Zhang, X.; Ding, L. 18% Efficiency organic solar cells. *Sci. Bull.* **2020,** *65,* 272–275.
[21] Cheng, P.; Zhan, X. Stability of organic solar cells: challenges and strategies. *Chem. Soc. Rev.* **2016,** *45,* 2544–2582.
[22] Burlingame, Q.; Ball, M.; Loo, Y.-L. It's time to focus on organic solar cell stability. *Nat. Energy* **2020,** *5,* 947–949.
[23] Mateker, W. R.; McGehee, M. D. Progress in Understanding Degradation Mechanisms and Improving Stability in Organic Photovoltaics. *Adv. Mater.* **2017,** *29,* 1603940.
[24] Wang, Y.; Lee, J.; Hou, X.; Labanti, C.; Yan, J.; Mazzolini, E.; Parhar, A.; Nelson, J.; Kim, J.-S.; Li, Z. Recent Progress and Challenges toward Highly Stable Nonfullerene Acceptor-Based Organic Solar Cells. *Adv. Energy Mater.* **2021,** *11,* 2003002.
[25] Guo, J.; Wu, Y.; Sun, R.; Wang, W.; Guo, J.; Wu, Q.; Tang, X.; Sun, C.; Luo, Z.; Chang, K.; Zhang, Z.; Yuan, J.; Li, T.; Tang, W.; Zhou, E.; Xiao, Z.; Ding, L.; Zou, Y.; Zhan, X.; Yang, C.; Li, Z.; Brabec, C. J.; Li, Y.; Min, J. Suppressing photo-oxidation of non-fullerene acceptors and their blends in organic solar cells by exploring material design and employing friendly stabilizers. *J. Mater. Chem. A* **2019,** *7,* 25088–25101.
[26] Liu, Z.-X.; Yu, Z.-P.; Shen, Z.; He, C.; Lau, T.-K.; Chen, Z.; Zhu, H.; Lu, X.; Xie, Z.; Chen, H.; Li, C.-Z. Molecular insights of exceptionally photostable electron acceptors for organic photovoltaics. *Nat. Commun.* **2021,** *12,* 3049.
[27] Park, S.; Son, H. J. Intrinsic photo-degradation and mechanism of polymer solar cells: the crucial role of nonfullerene acceptors. *J. Mater. Chem. A* **2019,** *7,* 25830–25837.
[28] Jiang, Y.; Sun, L.; Jiang, F.; Xie, C.; Hu, L.; Dong, X.; Qin, F.; Liu, T.; Hu, L.; Jiang, X.; Zhou, Y. Photocatalytic effect of ZnO on the stability of nonfullerene acceptors and its mitigation by SnO_2 for nonfullerene organic solar cells. *Mater. Horiz.* **2019,** *6,* 1438–1443.
[29] Liu, B.; Han, Y.; Li, Z.; Gu, H.; Yan, L.; Lin, Y.; Luo, Q.; Yang, S.; Ma, C.-Q. Visible Light–Induced Degradation of Inverted Polymer: Nonfullerene Acceptor Solar Cells: Initiated by the Light Absorption of ZnO Layer. *Sol. RRL* **2021,** *5,* 2000638.
[30] Park, S.; Kim, T.; Yoon, S.; Koh, C. W.; Woo, H. Y.; Son, H. J. Progress in Materials, Solution Processes, and Long-Term Stability for Large-Area Organic Photovoltaics. *Adv. Mater.* **2020,** *32,* 2002217.

[31] Speller, E. M.; Clarke, A. J.; Luke, J.; Lee, H. K. H.; Durrant, J. R.; Li, N.; Wang, T.; Wong, H. C.; Kim, J.-S.; Tsoi, W. C.; Li, Z. From fullerene acceptors to non-fullerene acceptors: prospects and challenges in the stability of organic solar cells. *J. Mater. Chem. A* **2019,** *7,* 23361–23377.

[32] Liu, Y.; Li, M.; Zhou, X.; Jia, Q.-Q.; Feng, S.; Jiang, P.; Xu, X.; Ma, W.; Li, H.-B.; Bo, Z. Nonfullerene Acceptors with Enhanced Solubility and Ordered Packing for High-Efficiency Polymer Solar Cells. *ACS Energy Lett.* **2018,** *3,* 1832–1839.

[33] Zhang, Z.; Yu, J.; Yin, X.; Hu, Z.; Jiang, Y.; Sun, J.; Zhou, J.; Zhang, F.; Russell, T. P.; Liu, F.; Tang, W. Conformation Locking on Fused-Ring Electron Acceptor for High-Performance Nonfullerene Organic Solar Cells. *Adv. Funct. Mater.* **2018,** *28,* 1705095.

[34] Liu, Y.; Li, M.; Yang, J.; Xue, W.; Feng, S.; Song, J.; Tang, Z.; Ma, W.; Bo, Z. High-Efficiency As-Cast Organic Solar Cells Based on Acceptors with Steric Hindrance Induced Planar Terminal Group. *Adv. Energy Mater.* **2019,** *9,* 1901280.